

An anchoring transition at surfaces with grafted liquid-crystalline chain molecules

Harald Lange^{†,‡} and Friederike Schmid[†]

[†] *Fakultät für Physik, Universität Bielefeld, 33615 Bielefeld, Germany*

[‡] *Institut für Physik, Universität Mainz, 55099 Mainz, Germany*

The anchoring of nematic liquid crystals on surfaces with grafted liquid crystalline chain molecules is studied by computer simulations and within a mean field approach. The computer simulations show that a swollen layer of collectively tilted chains may induce untilted homeotropic (perpendicular) alignment in the nematic fluid. The results can be understood within a simple theoretical model. The anchoring on a layer of mutually attractive chains is determined by the structure of the interface between the layer of chain molecules and the solvent. It is controlled by an interplay between the attractive chain interactions, the translational entropy of the solvent and its elasticity. A second order anchoring transition driven by the grafting density from tilted to homeotropic alignment is predicted.

PACS numbers: 61.30.Hn, 61.30.Vx

I. INTRODUCTION

Nematic liquid crystals are fluids of elongated or oblate particles, which lack translational order, but exhibit long-range orientational order^{1,2}: the molecular axes have a common preferred direction, the director. Surfaces and interfaces align the nearby molecules and thus favor certain director orientations in the bulk³. This phenomenon, known as anchoring, plays a key role in the design of liquid-crystal display devices^{4,5}. From a technological point of view, one is particularly interested in tailoring surfaces which orient a liquid crystal with an arbitrary, well-defined anchoring angle.

In practice, alignment layers are often produced by mechanical rubbing of a polymer coated surface. The technique is simple and successful, yet it has drawbacks: Low tilt angles between the director and the surface normal cannot be achieved easily, and the alignment mechanism is still not understood completely^{6,7}. As an alternative, Halperin and Williams have suggested to use swollen brushes of liquid crystalline polymers as alignment layers^{8–10}. Their idea was to create a competition between the alignment favored by the bare substrate and that enforced by the stretching of polymers in a dense brush. The interplay between the distortion energy of the solvent director field and the conformational entropy of the brush was predicted to trigger a second order anchoring transition between a phase with planar (homogeneous) alignment at low grafting densities and one with tilted alignment at higher grafting densities. The tilt angle can be tuned by adjusting the grafting density.

Subsequently, Peng, Johannsmann and Rühle have undertaken first steps towards an experimental realization of such a scenario^{11,12}. A “grafting-from” technique¹³ allowed to grow thick side-chain liquid crystalline polymer brushes from a substrate covered with surface-attached initiators. A competition as required by Halperin and

Williams can be set up by covering the surface between the grafting sites with alkyl chains, which favor homeotropic alignment on the bare substrate. The resulting anchoring behavior has not yet been investigated. However, preliminary miscibility studies have shown that the liquid crystalline brushes can only be swollen to a very limited extent by low molecular weight nematic compounds, even if the latter are chemically similar¹⁴. One would thus expect that the scenario is altered: The brush and the nematic bulk are presumably separated by an interface, which will contribute significantly to the anchoring properties of the alignment layer.

This aspect of surface anchoring on grafted liquid crystalline chains is explored in the present paper. We study brushes of chains which are too short or too stiff to develop hairpins and the like, and hence mainly follow the director profile. If they attract each other, such short chains exhibit collective tilt¹⁵. The contribution of the chain entropy to the free energy is of minor importance. Instead, the elastic energy of director distortions competes with a tendency of the chain ends at the surface of the chain layer to stand up, so that more solvent particles can intrude into the interfacial region. As we shall see, the interplay between these two factors leads to a novel anchoring transition between a phase with tilted alignment and one where the layer of grafted chains aligns the bulk vertically (homeotropic alignment), even though the chains inside of the layer are tilted. This is demonstrated with computer simulations and analyzed within a simple theoretical model.

Our paper is organized as follows: We discuss the simulation method and the relevant simulation results in section II. The theoretical model is introduced and analyzed in section III. We summarize and conclude in section IV.

II. MONTE CARLO SIMULATIONS

We have performed Monte Carlo simulations of a fluid of axially symmetric ellipsoidal particles with elongation $\kappa = \sigma_{\text{end-end}}/\sigma_{\text{side-side}} = 3$. The system was confined between two hard walls, to which chains of the same particles were attached at one end. The grafting points were on a regular square lattice. The simulations were conducted in the NPT ensemble, at constant temperature and pressure, and fixed number of particles. Two chain monomers and/or solvent particles with orientations \mathbf{u}_i , \mathbf{u}_j ($|\mathbf{u}| = 1$), whose centers are separated by a distance vector \mathbf{r}_{ij} , interact through the pair potential

$$V_{ij} = \begin{cases} 4\epsilon_0 (X_{ij}^{12} - X_{ij}^6) + \epsilon_0 & : X_{ij}^6 > 1/2 \\ 0 & : \text{otherwise} \end{cases} \quad (1)$$

Here $X_{ij} = \sigma_0/(r_{ij} - \sigma_{ij} + \sigma_0)$ is an inverse reduced distance and the shape function¹⁶

$$\sigma_{ij}(\mathbf{u}_i, \mathbf{u}_j, \hat{\mathbf{r}}_{ij}) = \sigma_0 \left\{ 1 - \frac{\chi}{2} \left[\frac{(\mathbf{u}_i \cdot \hat{\mathbf{r}}_{ij} + \mathbf{u}_j \cdot \hat{\mathbf{r}}_{ij})^2}{1 + \chi \mathbf{u}_i \cdot \mathbf{u}_j} + \frac{(\mathbf{u}_i \cdot \hat{\mathbf{r}}_{ij} - \mathbf{u}_j \cdot \hat{\mathbf{r}}_{ij})^2}{1 - \chi \mathbf{u}_i \cdot \mathbf{u}_j} \right] \right\}^{-1/2} \quad (2)$$

approximates the contact distance in the direction of $\hat{\mathbf{r}}_{ij} = \mathbf{r}_{ij}/r_{ij}$ of two ellipsoids with orientations \mathbf{u}_i and \mathbf{u}_j ¹⁶. The anisotropy parameter χ is defined as $\chi = (\kappa^2 - 1)/(\kappa^2 + 1)$. A hard core potential prevents the particles from penetrating the walls at $z = 0$ and $z = L_z$:

$$V_W(z) = \begin{cases} 0 & : d_z(\theta) < z < L_z - d_z(\theta) \\ \infty & : \text{otherwise} \end{cases}, \quad (3)$$

$$\text{with } d_z(\theta) = \sigma_0/2 \sqrt{1 + \cos^2(\theta) (\kappa^2 - 1)}.$$

The function $d_z(\theta)$ is the contact distance between the surface and an ellipsoid of elongation κ and diameter σ_0 oriented with an angle θ with respect to the surface normal.

Chain monomers are connected by bonds of length b , which are subject to a spring potential with an equilibrium length $b = b_0$ and a logarithmic cutoff at $|b - b_0| = b_s$.

$$V_S(b) = \begin{cases} -\frac{k_s}{2} b_s^2 \ln \left(1 - \frac{(b - b_0)^2}{b_s^2} \right) & : |b - b_0| < b_s \\ \infty & : |b - b_0| > b_s \end{cases} \quad (4)$$

The bonds are made stiff and coupled to the orientations of the monomers by virtue of a stiffness potential

$$V_A(\theta_1, \theta_2, \theta_{12}) = k_a [4 - \cos(\theta_1) - \cos(\theta_2) - 2 \cos(\theta_{12})], \quad (5)$$

which depends on the angles θ_1 and θ_2 between the orientation of a monomer and the adjacent bonds, and the

angle θ_{12} between the two bonds. The first bond of each chain is attached to one of the surfaces.

We chose the model parameters $k_s = 10\epsilon_0/\sigma_0^2$, $k_a = 10\epsilon_0$, $b_0 = 4\sigma_0$ and $b_s = 0.8\sigma_0$. The simulations were performed at the temperature $T = 0.5\epsilon_0/k_B$ and pressure $P = 3\epsilon_0/\sigma_0^3$. This corresponds to a state well in the nematic phase: The transition to the isotropic phase occurs at the pressure $P = 2.3\epsilon_0/\sigma_0^3$. The bulk number density was $\rho = 0.313/\sigma_0^3$.

We used a rectangular simulation box of size $L_{\parallel} \times L_{\parallel} \times L_z$ with periodic boundary conditions in the x and y direction and fixed boundary conditions in the z direction. The Monte Carlo moves included particle displacements, rescaling of the simulation box in the z direction (the lateral box size L_{\parallel} was kept constant in order to maintain a fixed grafting density), and a special variant of configurational biased Monte Carlo moves^{17,19}, in which chain monomers are turned into solvent particles and new chains are grown from the solvent. Details of this algorithm will be published elsewhere^{18,19}.

We have studied systems with roughly 2000 solvent particles (the numbers varied slightly in the different runs) and up to 242 chains of four monomers in simulation boxes of lateral size $L_{\parallel} = 12\sigma_0$. The length L_z of the boxes fluctuated with $L_z \approx 65\sigma_0$ at the highest grafting density. The walls orient the solvent particles parallel to the surface. We started from an initial configuration where particles all pointed into the x direction. This was achieved by applying a strong orienting field over roughly 50.000 Monte Carlo steps. After turning this field off, the system was equilibrated over at least 1 million Monte Carlo steps; data were then collected over 5 million or more Monte Carlo steps.

The results from these simulations for a range of grafting densities Σ will be presented in detail elsewhere²⁰. Here, we focus on the anchoring effect that is the subject of this paper. Figure 1 shows two configuration snapshots of systems at grafting densities $\Sigma = 0.34/\sigma_0^2$ and $\Sigma = 0.84/\sigma_0^2$. The grafted chains are tilted in both cases. At the lower grafting density $\Sigma = 0.34/\sigma_0^2$, the tilt propagates into the bulk of the film. At $\Sigma = 0.84/\sigma_0^2$, the orientation of the liquid crystal outside in the bulk is perpendicular to the surface, even though the chains still retain tilt.

One might suspect an equilibration problem. In order to exclude this possibility, we have prepared an initial configuration in which all particles are oriented in the z direction. It relaxes into the same structure as Fig. 1.

The effect can be characterized more quantitatively by inspection of local order parameter profiles. The order tensor of a system of n particles is defined by¹

$$\mathbf{Q} = \frac{1}{n} \sum_{i=1}^n \left(\frac{3}{2} \mathbf{u}_i \otimes \mathbf{u}_i - \frac{1}{2} \mathbf{I} \right), \quad (6)$$

where \mathbf{u}_i denotes the orientation of the particle i as above, \mathbf{I} the unity matrix, and \otimes the dyadic product.

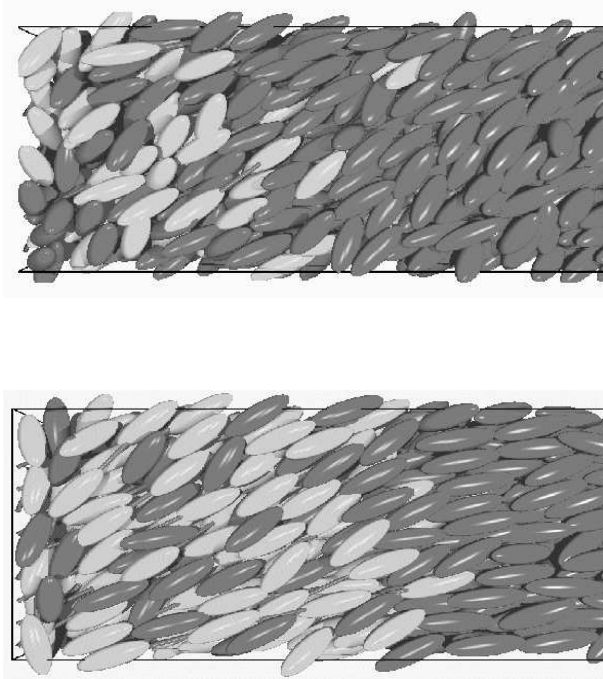


FIG. 1. Configuration snapshots (left half of the simulation box) at grafting densities $\Sigma = 0.34/\sigma_0^2$ and (top) and $\Sigma = 0.84/\sigma_0^2$ (bottom). Solvent particles are dark, and chain particles are bright.

The largest eigenvalue of this matrix is the nematic order parameter S (roughly 0.75 in the bulk of our system), and the corresponding eigenvector is the director \mathbf{n} . In order to obtain profiles of these quantities, we subdivide the system in the z direction into slabs of thickness $\delta z = 0.1\sigma_0$, and determine the order tensor in each slab. Note that the value of S is larger in a slab than in the bulk due to the small number of particles in each slab.

Figs. 2 a) and b) show averaged profiles of the order parameter and of the z -component of the director for the same grafting densities as in Fig. 1. The order parameter varies very little throughout the film; it is slightly larger in the chain region, due to the fact that chain monomers have less rotational freedom than solvent particles. The direction of alignment varies much more. Close to the surface, the particles are aligned parallel to the wall. However, the chains reorient the director within a few particle diameters from the surface. Then follows a region of slower changes, where the director gradually stands up. This region is restricted to the inside of the chain layer; further changes outside of the chain layer are small. In the case of $\Sigma = 0.84/\sigma_0^2$, the last monomers of the chains are almost perpendicular to the surface, even though the director is tilted inside of the chain region.

To characterize the chain layer further, Figs. 2 also

show the density of chains and the density of chain ends (end monomers). A few chain ends are located very close to the substrate at distances $z = 1 - 2\sigma_0$; they belong to chains which lie flat on the surface. The other chain ends are concentrated at the interface between the chain region and the bulk fluid. The higher the grafting density, the more efficiently the chain ends are expelled from the inside of the chain layer towards the chain-bulk interface.

Since the cell width $L_{\parallel} = 12\sigma_0$ is rather small, quantitative details of the curves shown in Fig. 2 are presumably subject to finite size effects. The simulations were very time consuming, and we were not able to consider different system sizes. In the following, we shall focus on the qualitative observation that the chains produce homeotropic alignment beyond a certain grafting density, even though they themselves remain tilted.

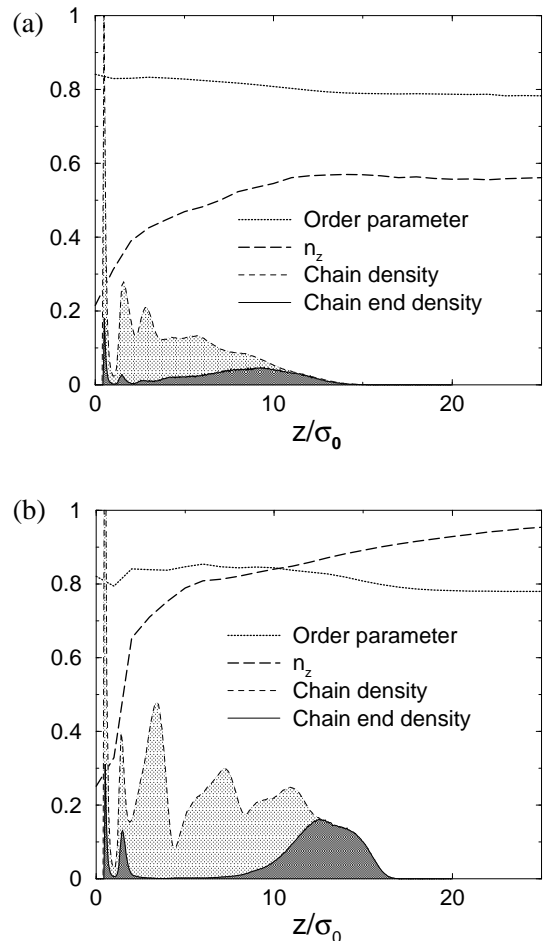


FIG. 2. Profiles of the order parameter S (dotted line) and the z component (dashed line) of the director \mathbf{n} as a function of the distance from the surface z for grafting densities $\Sigma = 0.34/\sigma_0^2$ (a) and $\Sigma = 0.84/\sigma_0^2$ (b). Also shown for comparison is the density profile of chain particles (thin dashed line) and the density of chain end particles (thin solid line) in units of $1/\sigma_0^3$.

III. A THEORETICAL MODEL

In this section, we shall propose a simple theoretical model for liquid crystalline chains in a nematic solvent which can explain the phenomenon reported in the previous section.

At first sight, the observation that the director orientation outside of the chain layer differs from that in the chain layer is surprising. The “interface” between the chain layer and the pure solvent seems to orient the particles in a homeotropic way. However, the origin of that anchoring force is not obvious. If one admits the existence of such an aligning force, one is left with the question why the chains are still tilted. In the scenario of Halperin and Williams⁸ the tilt is inherited from the bare substrate, which favors planar anchoring. In the simulations, the rapid director changes in the vicinity of the substrate suggest that the director orientation in the chain layer is largely decoupled from that at the substrate. Alternatively, collective tilt can be induced by attractive interactions between chains¹⁵. Such interactions can be mediated by solvent particles due to local packing effects, even if the direct interactions are purely repulsive²¹.

Our model is designed to investigate on a simplified level the effect of such an interaction. We describe the chains by smooth differentiable paths $\mathbf{R}(l)$ of length L (wormlike chains^{22,23}), which follow exactly the director field of the surrounding solvent: $d\mathbf{R}/dl = \mathbf{n}(\mathbf{R})$, and are attached to the surface at one end. The grafting density is measured in terms of a dimensionless area fraction ζ , which is defined as the grafting density times the cross section area of one chain. Fluctuations of the director are neglected. Moreover, we do not account for the possibility of hairpins^{24–26}.

The model has the following four key ingredients:

1. The elasticity of the nematic fluid.
2. The translational entropy of the solvent.
3. The interactions between the chains.
4. The anchoring energy of the substrate.

The elastic energy is given by the Frank free energy functional^{27–29}

$$\mathcal{F}_{\text{Frank}}\{\mathbf{n}(\mathbf{r})\} = \frac{1}{2} \int d\mathbf{r} \left\{ K_{11} [\nabla \cdot \mathbf{n}]^2 + K_{22} [\mathbf{n} \cdot (\nabla \times \mathbf{n})]^2 + K_{33} [\mathbf{n} \times (\nabla \times \mathbf{n})]^2 \right\}, \quad (7)$$

with the Frank elastic constants K_{11} (splay), K_{22} (twist) and K_{33} (bend).

The translational entropy of the solvent is calculated within the Flory-Huggins approximation^{30–32}

$$\mathcal{F}_{\text{solvent}}\{\Phi(\mathbf{r})\} = \frac{k_B T}{v_s} \int d\mathbf{r} (1 - \Phi) \ln(1 - \Phi). \quad (8)$$

Here k_B is the Boltzmann factor, T the temperature, v_s the volume occupied by a solvent particle, and $\Phi(\mathbf{r})$ the local volume fraction of chain monomers.

The excluded volume interactions between chains are incorporated by the constraint that $\Phi(\mathbf{r})$ must never exceed one. The attractive interactions are described by a quadratic free energy contribution,

$$\mathcal{F}_{\text{chains}}\{\Phi(\mathbf{r})\} = -\frac{v}{2} \int d\mathbf{r} \Phi^2, \quad (9)$$

where v is an effective interaction strength. Since the chains are monodisperse and have no hairpins, their ends are located on a smooth, well-defined surface. In the vicinity of that surface, the number of interacting neighbors of a monomer is reduced, which in turn reduces the interaction energy. We account for this by adding a correction term

$$\mathcal{F}_{\text{surface}}\{\Phi(\mathbf{r}); \mathbf{n}(\mathbf{r})\} = v \int_{\text{surface}} ds \Phi^2 \gamma(\Phi, \mathbf{n}, \mathbf{u}_s). \quad (10)$$

The integral $\int_{\text{surface}} ds$ runs over the surface of the chain layer, and \mathbf{u}_s denotes the unit vector in direction of the surface normal. The function γ integrates over the fraction of “missing” interaction energy in a region close to the surface. We take γ to be proportional to the thickness of the affected region, which we calculate as illustrated in Figure 3: $\gamma \propto a \sin(\theta)$, where θ is the angle between the monomer orientation \mathbf{n} and the surface normal \mathbf{u}_s , and a the distance between two neighbor chains, $a \propto 1/\sqrt{\Phi}$. This yields

$$\gamma(\Phi, \mathbf{n}, \mathbf{u}_s) = \hat{\gamma} \Phi^{-1/2} \sqrt{1 - (\mathbf{n} \cdot \mathbf{u}_s)^2}. \quad (11)$$

The proportionality constant $\hat{\gamma}$ depends on the form of the chain interactions and the actual chain packing at the surface, and is presumably of order 1.

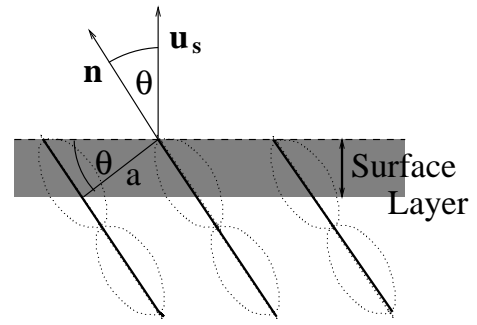


FIG. 3. Surface region of the chain layer where the interactions between chains are reduced. See text for explanation.

The free energy contribution (10), (11) turns out to be essential for the effect that we wish to study. On the other hand, the considerations which led to eqn. (11)

may seem somewhat crude and oversimplified. Therefore, we add some comments which justify an ansatz of the form (11) on more general grounds: In an anisotropic system, one clearly expects the missing neighbor contribution (10) at the surface of the chain layer to be anisotropic, i.e., to depend on the angle θ between the surface normal and the director. Since the chains are aligned along the director, interchain interactions take place in directions perpendicular to the director mainly. Hence fewer interactions are missing if the director is perpendicular to the surface, and the missing neighbor contribution should favor small θ . The ansatz (11), $\mathcal{F}_{\text{surface}} \propto \sin(\theta)$, ensures this in the simplest possible way. Other expressions which favor small θ lead to similar results.

Finally, the orienting effect of the bare substrate is described by a quadratic potential

$$\mathcal{F}_{\text{substrate}}\{\mathbf{n}(\mathbf{r})\} = W \int_{\text{substrate}} d\mathbf{s} (\mathbf{n} \cdot \mathbf{u}_s)^2. \quad (12)$$

The surface integral $\int d\mathbf{s}$ runs over the surface of the substrate. Other substrate-related free energy contributions, such as missing neighbor effects of the type (10) and solvent mediated interactions between the chains and the substrate are taken to be negligible compared to the anchoring energy (12). Furthermore, we neglect the internal stiffness of chains, and disregard the possibility that the elastic constants may vary locally and depend on the volume fraction occupied by the chains. These contributions can be incorporated in our model in a relatively straightforward way, but at the expense of having more model parameters. The results do not change qualitatively.

Since fluctuations are neglected, quantities vary only in the direction perpendicular to the surface, the z -direction, and the director \mathbf{n} does not rotate in the xy -plane. Inside of the chain layer, the local volume fraction $\Phi(z)$ of the chains is given by $\Phi(z) = \zeta/n_z(z)$. Outside of the chain layer, $\Phi(z)$ is zero and the director is constant. Hence the system can be described entirely in terms of the profile $n_z(z)$ inside of the chain layer. The free energy per surface area is given by

$$\begin{aligned} \mathcal{F}\{n_z(z)\} = & \int_0^H dz \left\{ \frac{1}{2} \left(\frac{dn_z}{dz} \right)^2 (K_{11} + K_{33} \frac{n_z^2}{1-n_z^2}) \right. \\ & + \frac{k_B T}{v_s} \left(1 - \frac{\zeta}{n_z} \right) \ln \left(1 - \frac{\zeta}{n_z} \right) - \frac{v}{2} \left(\frac{\zeta}{n_z} \right)^2 \left. \right\} \\ & + W n_z^2|_{z=0} + \hat{\gamma} v \sqrt{\zeta^3} \sqrt{\frac{1-n_z^2}{n_z^3}}|_{z=H}. \quad (13) \end{aligned}$$

The height H of the chain layer is determined implicitly by the requirement $L = \int_0^H dz/n_z(z)$.

For practical calculations, it is convenient to perform the variable transformation $dl = dz/n_z(z)$, i.e., to consider variations along the chains rather than variations in the z -direction. Furthermore, we define the units of length and energy³³ such that $(K_{11} + K_{33})/2 = 1$

and $k_B T/v_s = 1$, and introduce the notation $\delta K = (K_{33} - K_{11})/(K_{33} + K_{11})$. The free energy per surface area is then expressed as a functional of the profile $\theta(l) = \arccos(n_z(l))$ of the angle θ between \mathbf{n} and the surface normal:

$$\begin{aligned} \mathcal{F}\{\theta(l)\} = & \int_0^L dl \left\{ \frac{1}{2} C(l) \left(\frac{d\theta}{dl} \right)^2 + U(\theta) \right\} \\ & + W \cos^2(\theta)|_{l=0} + \hat{\gamma} v \sqrt{\zeta^3} \frac{\sin(\theta)}{\sqrt{\cos^3(\theta)}}|_{l=L}, \quad (14) \end{aligned}$$

with

$$C(\theta) = \frac{1}{\cos(\theta)} (1 + \delta K \cos(2\theta)) \quad (15)$$

$$U(\theta) = \zeta \hat{U} \left(\frac{\cos(\theta)}{\zeta} \right) \quad (16)$$

$$\text{and} \quad \hat{U}(x) = (x-1) \ln \left(1 - \frac{1}{x} \right) - \frac{v}{2x}.$$

Minimizing this functional yields the Euler-Lagrange equation

$$C \frac{d^2 \theta}{dl^2} + \frac{1}{2} \left(\frac{d\theta}{dl} \right)^2 \frac{dC}{d\theta} - \frac{dU}{d\theta} = 0. \quad (17)$$

and the boundary conditions

$$\begin{aligned} l=0 : \quad & C(\theta) \frac{d\theta}{dl} = -2W \cos(\theta) \sin(\theta) \\ & \text{or} \quad \theta = \arccos(\zeta) \end{aligned} \quad (18)$$

$$\begin{aligned} l=L : \quad & C(\theta) \frac{d\theta}{dl} = -\hat{\gamma} v \sqrt{\zeta^3} \frac{1 + 3/2 \tan^2(\theta)}{\sqrt{\cos(\theta)}} \\ & \text{or} \quad \theta = 0. \end{aligned} \quad (19)$$

Eqn. (17) describes the trajectory of a particle in space θ and time l with a position dependent mass $C(\theta)$, which moves in the potential $-U(\theta)$. The boundary conditions pull the particle in the direction of large θ at $l=L$ and in the direction of small θ at $l=0$. Hence the profile of θ decreases monotonically with l . The anchoring angle on the chain layer is given by $\theta(L)$.

The properties of the model are most easily discussed in the limit of long chains, $L \rightarrow \infty$. The two boundaries of the chain layer at $l=0$ and $l=L$ are then decoupled, and there exists a region inside of the chain layer in which $\theta(l)$ is constant, $\theta(l) \equiv \bar{\theta}$. The stationary angle $\bar{\theta}$ is the angle where $U(\theta)$ has its minimum. It depends on the grafting density ζ and the chain interaction parameter v . If $v > 1$, the chains exhibit a continuous transition from an untilted state at large ζ to a tilted state at $\zeta < \zeta_c(v)$, where $\zeta_c(v)$ is determined by the implicit equation

$$v = -\frac{2}{\zeta_c(v)^2} \{ \zeta_c(v) + \ln[1 - \zeta_c(v)] \}. \quad (20)$$

In the vicinity of the phase transition, at $\zeta \approx \zeta_c(v)$, the potential $U(\theta)$ can be expanded like

$$U(\theta) = \text{const.} - \frac{1}{2}(\zeta_c - \zeta) b(\zeta_c) \theta^2 + \frac{1}{8} \zeta_c b(\zeta_c) \theta^4 \quad (21)$$

with $b(\zeta) = (2 - \zeta)/(1 - \zeta) + 2/\zeta \ln(1 - \zeta)$, and the minimum is found at

$$\bar{\theta} = \sqrt{2(\zeta_c - \zeta)/\zeta_c}. \quad (22)$$

A necessary criterion for the validity of the expansion is obviously $\Phi = \zeta/\cos(\bar{\theta}) < 1$, which is fulfilled if

$$\zeta_c - \zeta < 2\zeta_c \arccos^2(\zeta_c). \quad (23)$$

Far from the transition, $U(\theta)$ takes its minimum close to the maximum value of θ at $\cos(\bar{\theta})/\zeta \approx 1$ and one obtains

$$U(0) - U(\bar{\theta}) = (1 - \zeta)[\ln(1 - \zeta) + v\zeta/2]. \quad (24)$$

In the case $L \rightarrow \infty$, the anchoring angle $\theta(L)$ of the nematic film at the surface of the chain layer does not depend on the anchoring strength W of the substrate. Exploiting the integration constant of the Euler-Lagrange equation (17), $U(\theta) - \frac{1}{2}C(\theta)(\frac{d\theta}{dl})^2 \equiv \text{const.} = U(\bar{\theta})$, one can rewrite the boundary condition (19) at $l = L$ as

$$U(\theta(L)) - U(\bar{\theta}) = g(\theta) \quad \text{or} \quad \theta(L) = 0. \quad (25)$$

$$\text{with } g(\theta) = 2\hat{\gamma}^2 v^2 \zeta^3 \frac{(1 + 3/2 \tan^2(\theta))^2}{1 + \delta K \cos(2\theta)}$$

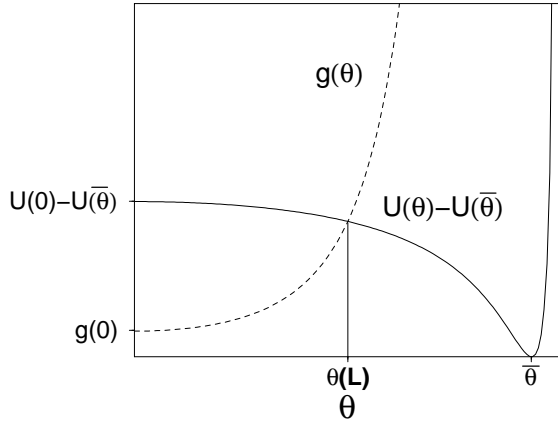


FIG. 4. Graphical solution of Eqn. (25). The anchoring angle $\theta(L)$ is given by the point where $g(\theta)$ (dashed line) and $U(\theta) - U(\bar{\theta})$ (solid line) cross. If $g(0)$ is larger than $U(0) - U(\bar{\theta})$, the anchoring angle is zero. (The parameters leading to this particular plot were $\zeta = 0.1, v = 1.7, \hat{\gamma} = 0.5, \delta K = 0$. Units are defined in the text³³).

The problem can be solved graphically as sketched in Fig. 4. Since $g(\theta)$ grows monotonically for all $\delta K < 1$, the curves $g(\theta)$ and $U(\theta) - U(\bar{\theta})$ cross at most at one point in the region $\theta < \bar{\theta}$. If such a point exists, it defines the anchoring angle $\theta(L)$. Otherwise, the case $\theta(L) = 0$ applies and the anchoring is homeotropic. The transition between homeotropic and tilted anchoring is continuous. The grafting density at the transition $\zeta^*(v)$ can be calculated by solving $U(0) - U(\bar{\theta}) = g(0)$ for a given interaction parameter v . If v is small, $\zeta^*(v)$ is close to the tilting transition $\zeta_c(v)$ of the chains, and Eqn. (22) applies. The tilt angle $\bar{\theta}^*$ of the chains at the transition can be approximated by its asymptotic value at small grafting densities $\zeta^*(v) \xrightarrow{v \rightarrow 1} 0$. Using Eqns. (20) and expanding $\cos(\bar{\theta}^*)$ in powers of $\bar{\theta}^*$, one obtains after some algebra

$$\zeta^*(v) \sim \zeta_c(v)/(1 + 2\hat{\gamma}\sqrt{3/(1 + \delta K)}). \quad (26)$$

At large v , ζ^* is far from ζ_c and Eqn. (24) leads to

$$\zeta^*(v) \sim \sqrt{1 + \delta K}/(2\hat{\gamma}\sqrt{v}). \quad (27)$$

Fig. 5 shows two examples of phase diagrams for the parameter values $\hat{\gamma}/\sqrt{1 + \delta K} = 0.5$ and 0.1 . We expect that typical values of $\hat{\gamma}/\sqrt{1 + \delta K}$ are in that range. At high grafting density ζ and low chain interaction parameter v , the chains stand upright, perpendicular to the surface. The thin line marks the continuous transition $\zeta_c(v)$ to a phase where they tilt collectively. However, the orientation of the director outside of the chain layer still remains perpendicular. Only at grafting densities below a second critical value $\zeta^*(v) < \zeta_c(v)$ (thick line) do the chains induce tilted alignment in the bulk of the nematic fluid.

In agreement with the observations from computer simulations reported in the previous section II, we thus find a region in $\zeta - v$ space where the chains are tilted, but nevertheless align the solvent in a homeotropic way. The size of that region increases with $\hat{\gamma}$, i.e., with the amplitude of the (anisotropic) missing neighbor effect at the surface of the chain layer. It is bounded by two continuous phase transitions - one at high grafting density to a phase where both the chains and the adjacent fluid are untilted, and one at low grafting density to a phase where they are both tilted.

So far we have discussed this phenomenon for the limit of long chains, $L \rightarrow \infty$. In systems with shorter chains, the scenario remains qualitatively similar. If the anchoring on the bare substrate is planar ($W > 0$ in Eqn. (12)), the sharp tilting transition in the chain region is replaced by a smoother crossover from distinctly tilted to roughly perpendicular chain orientation³⁴, and the anchoring transition shifts to higher grafting densities. One still finds a region where markedly tilted chains align the nematic solvent in a homeotropic way.

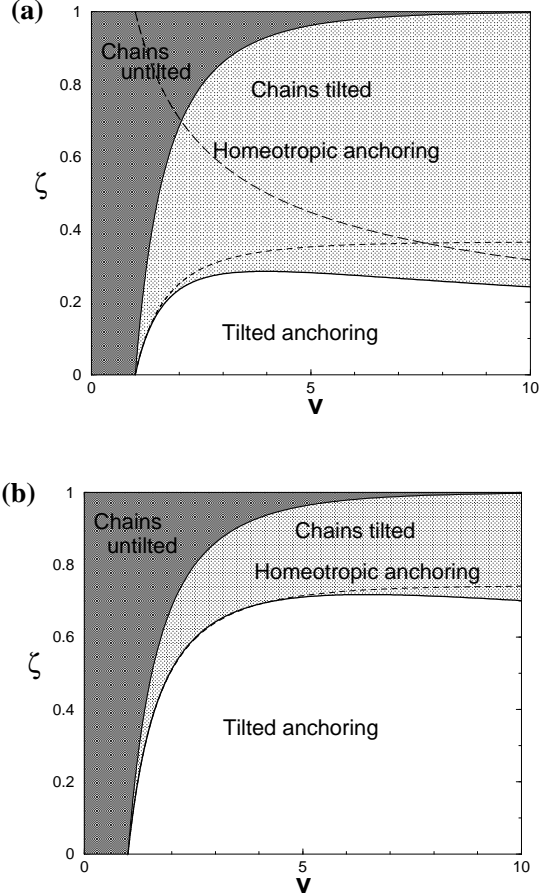


FIG. 5. Phase diagrams in $v - \zeta$ space (chain interactions vs. grafting density) for $\hat{\gamma}/\sqrt{1+\delta\bar{K}} = 0.5$ (a) and $\hat{\gamma}/\sqrt{1+\delta\bar{K}} = 0.1$ (b). Thin solid lines indicate tilting transition in the chain region, and thick solid line the anchoring transition in the nematic fluid. Short dashed line indicates the approximation (26) and long dashed line the approximation (27) (outside of the frame in the case of (b)). Units are defined in the text³³.

IV. SUMMARY AND DISCUSSION

To summarize, we have described a new type of anchoring transition on grafted layers of main-chain liquid-crystalline chain molecules. It is driven by the competition between attractive chain interactions, the translational entropy of the nematic solvent in a region close to the surface of the chain layer, and the elastic energy of the nematic fluid which opposes rapid director changes. Inside of the chain layer, the chain interactions make the chains tilt collectively. Close to the surface, the interactions are reduced, and an increased number of solvent particles enters and swells the chains. As a result, chain ends in the surface region stand up. The anchoring angle imposed by the chains on the adjoining nematic fluid

is thus smaller than the actual tilt angle of the chains. Above a critical grafting density ζ^* , it drops to zero, despite the fact that the chains are still tilted. We have observed this effect in computer simulations of a model system with swollen grafted chains, and rationalized it in terms of a simple theoretical model.

The new anchoring transition is controlled by the grafting density of the chains. In that sense, it is similar to that discussed by Halperin and Williams^{8–10}. However, the phase transition and the underlying mechanism is very different. In the case studied by Halperin and Williams, the chains are long and flexible enough to support many hairpins. The solvent is taken to be very good, i. e., chain monomers effectively repel each other. The transition is driven by an interplay between the conformational entropy of the chains, the anchoring force of the substrate on the solvent, and the elastic energy in the brush. The transition connects a phase with planar anchoring and one with tilted anchoring.

In the present paper, we consider a different regime: The chains are shorter or stiffer, they have no hairpins, and their conformational entropy is negligible. The solvent is not good, chains effectively attract each other and there exists a well-defined interface between the chain layer and the solvent. The anchoring behavior is controlled by the structure of that interface. The influence of the bare substrate is minor. The transition connects a phase with tilted anchoring and one with perpendicular anchoring.

One might ask whether there could be a second transition between planar and tilted anchoring, at a lower grafting density, which would resemble that discussed by Halperin and Williams. Our theoretical model does not predict such a transition. In the simulations, the situation is more complicated. The data indicate the presence of a first order transition, which has nothing to do with hairpins, but is still related to the organization of the chains. This will be described in detail in a separate publication^{18,20}.

Experimentally, one finds that liquid crystalline polymers are not swollen very well by nematic solvents¹⁴. We thus believe that our effect can be observed in real systems. The grafting density must be high to achieve low anchoring angles θ , on the other hand, the chains need not be much longer than their persistence length. Moreover, our results indicate that the grafting density required for the transition decreases with decreasing solvent quality. Brushes with high grafting densities can be prepared with the “grafting from” technique developed by R  he et al¹³. This technique has been used in the experiments of Peng et al^{11,12} mentioned in the introduction. However, Peng et al studied brushes with liquid crystalline side chains, where the mesogenic units are preferably oriented perpendicular to the backbone of the chains. The swelling of the brush in the surface region thus promotes planar anchoring, and no transition to homeotropic anchoring can be expected. The effect discussed in the present paper will presumably transpire

in a similar experiment with short main-chain liquid-crystalline polymers.

One necessary requirement is of course that the orientation of the chains is homogeneous. This turned out to be a problem experimentally¹¹, the brushes tend to exhibit planar multidomains. However, recent work indicates that an appropriate treatment of the bare substrate before growing the brush can force the chains into one monodomain¹². If brushes could be grown with grafting densities close to the transition density ζ^* , it would be possible to prepare surfaces which anchor the solvent at any given small tilt angle θ^* . This would potentially have applications in the design of liquid crystal display devices.

Future theoretical work will have to study in more detail the chain length dependence. The theory presented here has been devised for long chains – for example, they have been described by homogeneous strings – but the chains in the simulations were very short with only four monomer units. Chains in real brushes are usually polydisperse. The influence of polydispersity on the anchoring behavior is not clear. Thus far the analytical model calculations have disregarded the possibility of lateral structure and lateral fluctuations. These will certainly become important for polydisperse brushes and more generally at low grafting densities.

ACKNOWLEDGMENTS

We thank M. P. Allen and K. Binder for useful discussions, and for allowing us to perform a major part of the simulations on the computers of the university of Bristol and the university of Mainz. We have also benefitted from stimulating interactions with D. Johannsmann, J. R  he and A. Halperin. This work was funded by the German Science Foundation (DFG).

¹ P.-G. de Gennes and J. Prost, *The Physics of Liquid Crystals* (Oxford University Press, Oxford, 1995).

² S. Chandrasekhar, *Liquid Crystals* (Cambridge University Press, Cambridge, 1992).

³ B. Jerome, Rep. Progr. Phys. **54**, 391 (1991).

⁴ B. Bahadur (edt.) *Liquid crystals and uses*, World Scientific, Singapore (1990).

⁵ M. Schadt, Ann. Rev. Mater. Science, **27**, 305 (1997).

⁶ M.F. Toney, T.P. Russell, J.A. Logan, H. Kiguchi, J.M. Sands, S K. Kumar, Nature, **374**, 709 (1995).

⁷ N. L. Abbott, Curr. Opin. Coll. Interf. Science **2**, 76 (1997).

⁸ A. Halperin, D. R. M. Williams, Europhys. Lett. **21**, 575 (1993).

⁹ A. Halperin, D. R. M. Williams, J. Physics: Cond. Matt. **6**, A297 (1994).

¹⁰ A. Halperin, D. R. M. Williams, Ann. Rev. of Mat. Science **26**, 279 (1996).

¹¹ B. Peng, D. Johannsmann, J. R  he, Macromolecules **32**, 6759 (1999).

¹² B. Peng, J. R  he, D. Johannsmann, Adv. Mater. **12**, 821 (2000).

¹³ O. Prucker, J. R  he, Macromolecules **31**, 592 (1998); *ibid*, 602 (1998).

¹⁴ F. Benmouna, B. Peng, J. R  he, D. Johannsmann, Liqu. Cryst. **26**, 1655 (1999).

¹⁵ F. Schmid, D. Johannsmann, A. Halperin, J. de Physique **6**, 1331 (1996).

¹⁶ B. J. Berne and P. Pechukas, J. Chem. Phys. **56**, 4213 (1975).

¹⁷ D. Frenkel, B. Smit, *Understanding Molecular Simulation*, Academic Press, San Diego (1996).

¹⁸ H. Lange, Dissertation Universit  t Mainz (2001).

¹⁹ H. Lange, F. Schmid, submitted to Comp. Phys. Comm. (2001).

²⁰ H. Lange, F. Schmid, manuscript in preparation.

²¹ M. M  ller, F. Schmid, in *Annual Reviews in Computational Physics* VI, pp. 59, D. Stauffer edt., World Scientific, Singapore (1999).

²² O. Kratki, G. Porod, Recl. Trav. Chim. **68**, 1106 (1949).

²³ N. Saito, K. Takahashi, Y. Yuniki, J. Phys. Soc. Jpn. **22**, 219 (1967).

²⁴ P. G. de Gennes, in *Polymer Liquid Crystals*, A. Ciferri, W. R. Krigbaum, R. Meyer eds. (Academic Press, New York, 1982).

²⁵ M. Warner, J. M. F. Gunn, A. B. Baumg  rtner, J. Phys. A **18**, 3007 (1985).

²⁶ A. L. Khodolenko, T. A. Vilgis, Phys. Rev. E **52**, 3973 (1995).

²⁷ C. Oseen, Trans. Faraday Soc. **29**, 883(1933).

²⁸ H. Z  cher, Trans. Faraday Soc. **29**, 945(1933).

²⁹ F. C. Frank, Discuss. Faraday Soc. **25**, 19 (1958).

³⁰ P. J. Flory, J. Chem. Phys. **9**, 660 (1941).

³¹ H. L. Huggins, J. Chem. Phys. **9**, 440 (1941).

³² P. J. Flory, *Principles of Polymer Chemistry* (Cornell University Press, Ithaca, New York, 1971).

³³ The length unit is $[x] = \sqrt{v_s/k_B T (K_{33} + K_{11})/2}$, and the energy unit is $[E] = k_B T/v_s [x^3]$.

³⁴ In the case of homeotropic substrate anchoring, $W < 0$, a sharp tilting transition in the brush is still possible.